Guardiola, C.; Pla Moreno, B.; Blanco-Rodriguez, D.; Bares Moreno, P. (2014). Cycle by Cycle Trapped Mass Estimation for Diagnosis and Control. SAE International Journal of Engines. 7(3):1-9. doi:10.4271/2014-01-1702.

Cycle by cycle trapped mass estimation for diagnosis and control

C. Guardiola, B. Pla, D. Blanco-Rodriguez, P. Bares
CMT-Motores Térmicos, Universitat Politècnica de València

contact: Carlos Guardiola; carguaga@mot.upv.es

Abstract

The development of one cycle resolution control strategies and the research at HCCI engines demands an accurate estimation of the trapped mass. In contrast to current methods for determining the mass flow, which are only able to determine averaged values of the flow entering the cylinders, the present paper proposes a methodology based on the in-cylinder pressure resonance. The determination of such frequency allows inferring the cylinder mass with one cycle resolution. In addition, the method permits determining error metrics based on the mass conservation principle. Validation results for a reactivity controlled compression ignition (RCCI) engine equipped with electrohydraulic variable valve timing (VVT) are presented to illustrate the performance of the method.

Introduction

Trapped mass estimation is currently achieved by the estimation of different inputs: air mass by flow sensors, fuel mass by injection calculations, and residual gases through different assumptions.

The air measurement can be improved by observers [1,2], Kalman filters [3,4,5], mean value models [6,7], or data-driven methods [8], which improve the estimation of the air mass flow. The injected fuel mass estimation provided by the electronic control unit (ECU), despite its possible deviations [9, 10], has in most cases the required precision. The external exhaust recirculated gases (EGR) are estimated from exhaust and intake CO_2 concentration. However, the internal residual gases cannot be sensed properly and different assumptions are used, e.g. valve flow methods calculate the residual trapped mass by physical valve models [11,12,13], while Δp method relies on polytropic compression [14].

Nevertheless, none of these methods is suitable for estimating accurately the trapped mass on transient operation: On the one hand, flow methods, which make use of averaged values, cannot estimate instantaneously the trapped mass with precision, then leading to important errors during transient operation. On the other hand, the assumption of adiabatic behavior or the use of unknown in-cylinder parameters for the models, such as the temperature of the gases, results in serious errors on the estimated trapped mass [15].

The present paper harnesses the relation between the speed of sound and the resonance frequency to develop a method for estimating the mass. A method based on the resonance permits obtaining a mass estimation with cycle-to-cycle resolution, just relaying on the pressure signal, a volume calculation and a composition assumption. Even more, it is possible to calculate the cylinder mass variations in poly-cylindrical engines.

Only R. Hickling et al., in the early 80's, tried to use the resonance phenomenon in order to estimate in-cylinder variables, particularly the bulk temperature [16,17]. Herein, unlike the works developed by R. Hickling et al., the authors have made use of time-frequency signal processing [18] for an accurate estimation of the resonance frequency. Moreover, the possibility of obtaining many measures during a cycle permits an error metric based on the mass conservation principle. The method was tested under specific transient tests and compared with current methods on different stationary points, varying the trapped mass and the injection strategy.

The paper is organized as follows. First, the main working principles of the method are explained: the state of the art in the study of the pressure resonance, followed by the singularities of the proposed method. Once the methodology is known, the RCCI engine used to test the method is described. Following, the tests developed are presented and the results obtained are commented: transient steps will evidence the one cycle resolution, while stationary measured points will demonstrate its accuracy. Finally, last section is aimed to highlight the main contributions of the method.

Methodology

Pressure Resonance

In-cylinder pressure resonance is a well-known phenomenon, extensively studied along the last decades in order to detect knock and reducing noise [19, 20, 21]. Pressure resonance consists on high frequency (few kHz) oscillation caused by pressure waves on the cylinder (figure 1).

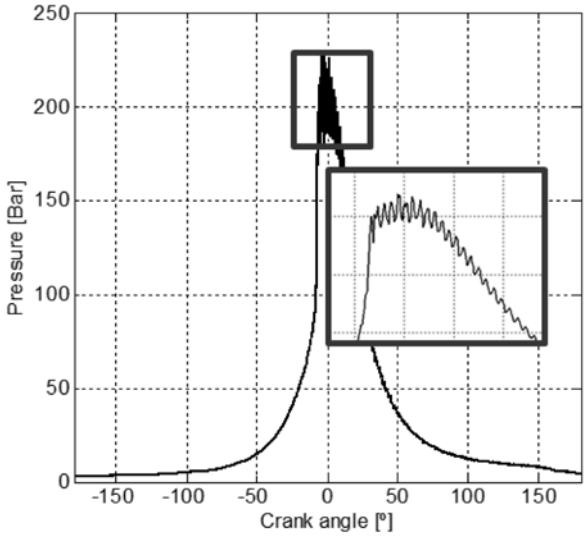

Figure 1. Pressure signal of a cycle with knock

Most of pressure resonance works use the approach stated by Draper [22] to estimate the resonance frequencies by a cylindrical chamber assumption: Draper solved the wave equation with Bessel functions for a cylindrical geometry. He ended up with (1), which relates the resonance frequency ($f_{i,j}$) with the cylinder diameter (D), the speed of sound (a) and a Bessel constant ($B_{i,j}$), tabbed at table 1. The axial modes can be neglected because the frequencies associated to h (heigh of the combustion chamber) are too high.

$$f_{i,j} = a\sqrt{\frac{{B_{i,j}}^2}{(\pi D)^2} + \frac{g^2}{(2h)^2}} = \frac{aB_{i,j}}{\pi D} \qquad (1)$$

Table 1. First radial modes for a cylindrical chamber

	$B_{i,0}$	$B_{i,1}$
$B_{0,j}$	3.832	7.016
$B_{1,j}$	1.841	5.332
$B_{2,j}$	3	6.75

Draper's equation is normally used to estimate a reference frequency to capture (knock detection) or to eliminate the resonance (combustion diagnosis). To these ends, it is used a pass-band or a low-pass filter with few kHz as margin [21].

Although far from the TDC the cylindrical solution is valid, near the TDC this solution is not precise in common reciprocating engines as consequence of the singular bowl geometries [23]. Figure 2 compares the cylindrical resonance frequencies stated at (1) with the experimental frequencies obtained at a cylinder with bowl: although there is a frequency variation due to temperature, the resonance frequencies change even more. The discrepancies between (1) and the results obtained are presumably caused by the geometry shift between a cylinder dominated geometry (far from the TDC) and a bowl dominated geometry (near the TDC).

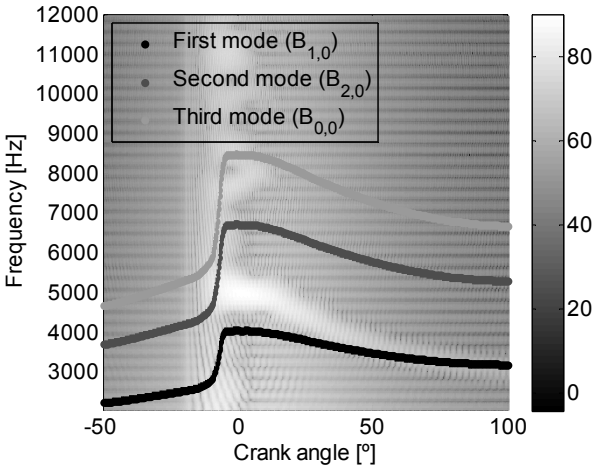

Figure 2. Cylindrical resonance modes over a spectrogram in a cylinder with bowl

A possibility for correcting the bowl, is applying pre-calibrated crank angle varying constants for the bowl (2). In this manner, although a cylindrical solution is being used, the geometry shifting errors are taken into account by specific constants ($B_{i,j}{}'$). The main drawback of this method is the calibration of constants, because it must be done with previous data when the mass must be precisely known.

$$B_{i,j}{}' = f(\alpha) = \frac{\pi D f_{i,j}}{a} \qquad (2)$$

Resonance frequencies identification

Once the relation between the resonance frequencies and the speed of sound is calibrated (2), the opposite process can be done to obtain the speed of sound during a cycle (3). In both processes, the frequency calculation is crucial for the final accuracy of the measurement.

$$a = \frac{\pi D f_{i,j}}{B_{i,j}} \qquad (3)$$

The authors have used the discrete Short Time Fourier Transform (STFT) with zero padding to identify the frequency components of the signal: the STFT is based on windowing the pressure signal at different crank angle positions in order to have crank angle resolution while applying zero-padding permits improving the frequency resolution [18].

Figure 3 shows the output obtained by using a *Blackman-Harris* window of 25 degrees. Although the identification of all modes is possible, only the first one appears neatly in all the range.

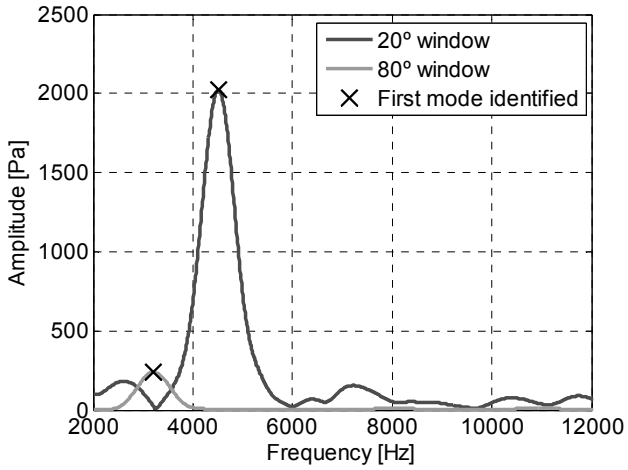

Figure 3. Resonance frequency identification at 20º and 80º (1200 rpm, 50% load, one diesel injection RCCI combustion).

In order to have an appropriate resonance identification, the excitation must be sufficient. Several resonance quantification works [24, 25] relate the resonance amplitude to the pressure gradient. Consequently, although this method can have problems when used with conventional combustions, it is fully adequate for new combustion modes engines which are nowadays investigated and need combustion diagnosis tools [26].

Problem formulation

The determination of the trapped mass can be solved through the following equations:

$$a = \frac{\pi D f_{i,j}}{B_{i,j}} \tag{4}$$

$$a^2 = \gamma R T \tag{5}$$

$$pV = mRT \tag{6}$$

$$R = f(Y_x) \tag{7}$$

$$C_v = \frac{R}{\gamma - 1} = f(Y_x, T) \tag{8}$$

Actually, the mass variation due to composition (Y_x) is bounded below 3.5% (appendix 1). Accordingly, a rough estimation of a constant composition (by assuming 50% of burnt products) is expected to have errors associated that are lower than 1%. To cope with lower errors, the composition can be inferred by using polynomial expression for R and γ and assuming complete combustion:

1. The dependency of R and γ with the temperature and the composition (7 and 8) can be calculated as in [27]. M. Lapuerta et al. divided the gas in 3 species (fuel, air and burnt gases). They considered the temperature effect over R negligible and obtained polynomial correlations with temperature for estimating C_{vf}, C_{va} and C_{vb}.

$$R = R_f Y_f + R_a Y_a + R_b Y_b \tag{9}$$

$$C_v = C_{vf}(T) Y_f + C_{va}(T) Y_a + C_{vb}(T) Y_b \tag{10}$$

2. The composition can be inferred by using MFB models, e.g. Rassweiller and Withrow model [28], assuming complete combustion and using initial known variables, such as the injected fuel ($m_{f,in}$) or the air admitted ($m_{a,ret}$). In this manner, the only unknown is the residual gasses, which can be obtained as a function of the total mass. A scheme of the composition calculation is represented at figure 4.

Anyway, the system is solvable and a polynomial expression of the form (11) can be solved by any iterative method, such as bisection or fixed-point. Therefore, at every cycle, many mass estimations can be obtained at different crank angle positions.

$$\boldsymbol{f}(\boldsymbol{m}) = \boldsymbol{0} \tag{11}$$

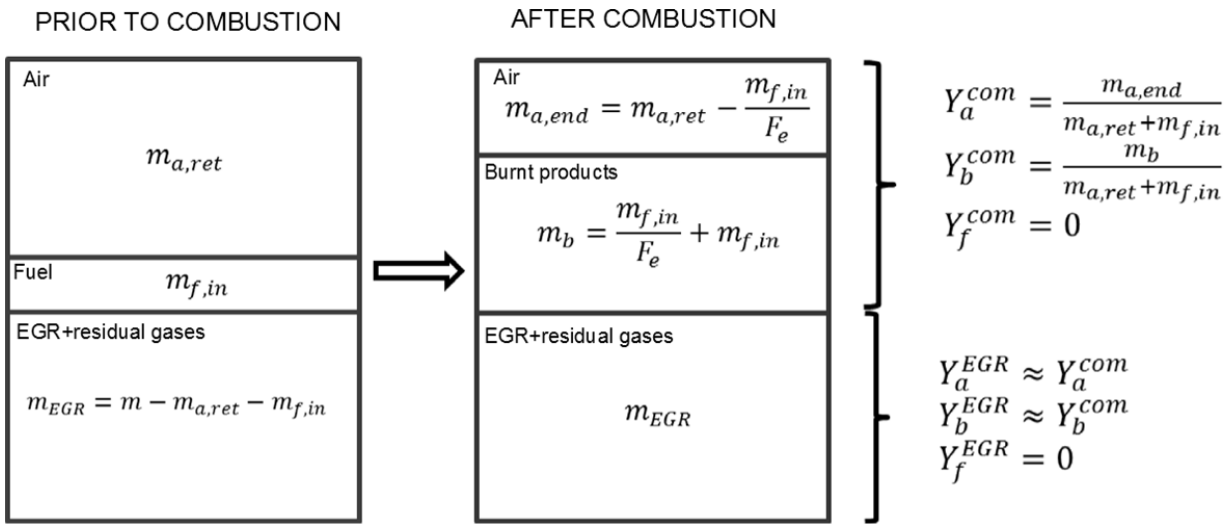

Figure 4. Scheme of combustion assuming complete combustion

Experimental set-up

The tests were developed on a mono-cylindrical RCCI experimental engine. The engine was equipped with gasoline port injection and diesel direct injection, allowing multiple diesel injections. EGR facilitated the control of the engine over different configurations, while electrohydraulic variable valve timing (VVT) permitted controlling the valves to change the mass instantaneously at transient tests. The pressure was sensed by a *Kistler 6125c* sensor and processed by a NI-PXI acquisition system. The main characteristics of the engine are summarized in table 2.

Table 2. Main engine characteristics.

Displaced volume	1806 cc
Engine speed	1200
Stroke	152 mm
Bore	123.6 mm
Connecting Rod	225 mm
Number of Valves	4
Combustion mode	RCCI-Diesel
Pressure samples/degree (s_n)	5
In-cylinder pressure sensor	Kistler 6125c

The test campaign was designed to prove the accuracy of the measurement and the transient response of the method. Consequently, two type of tests were made:

- Steady state: 54 different points were tested under different injection strategies (diesel, RCCI one injection and RCCI two injections) and different loads (ranging from 25% to 100%).
- Valve steps: Sudden changes at valve configuration permits varying instantaneously the trapped mass. The tests consisted on varying the valve configuration at a stationary point and in measuring the mass.

Even though all tests were conducted at the same engine speed due to test bench requirements, the only limitation of the method is the Nyquist frequency ($F_s/2 \geq f_{1,0}$). Then, if the pressure measurement is crank angle based, the frequency acquisition (F_s) depends on the engine speed and the encoder resolution:

$$F_s = \frac{360\, n}{60} s_n \leq 2\, f_{1,0} \quad (12)$$

Considering the maximum range of the resonance frequency for this engine (up to 6 kHz), and a encoder resolution of 5 samples/deg, the minimum admissible engine speed would be 400 rpm, which is clearly above idle speed.

The auxiliary method employed to calibrate and evaluate the resonance method is based on the direct measurement of the air mass flow through hot wire anemometry, the determination of EGR by means of CO2 balance in the intake manifold, the measurement of the blow-by using the orifice measuring principle, and the determination of the fuel mass flow by a fuel balance. An emptying-and-filling model as in [11, 12, 13] is used for solving the flow through the engine valves and for estimating the residual gas fraction and short circuit.

Results and discussion

Method calibration

As stated before, the method needs from constants calibration over past data. The mass calculated and sensed at a few known operation points was used to identify the Bessel constants of the first mode:

$$B' = \frac{\pi D f_{1,0} \sqrt{m}}{\sqrt{\gamma p V}} \quad (13)$$

Figure 5 shows the estimates obtained for the Bessel constant over many cycles at different operation points. The selected operation points come from a test campaign where the

combustion center (CA50) was maintained between -7 and 7 CAD before TDC. Test shown in Figure 5 include operation points ranging from 25% to 100% load.

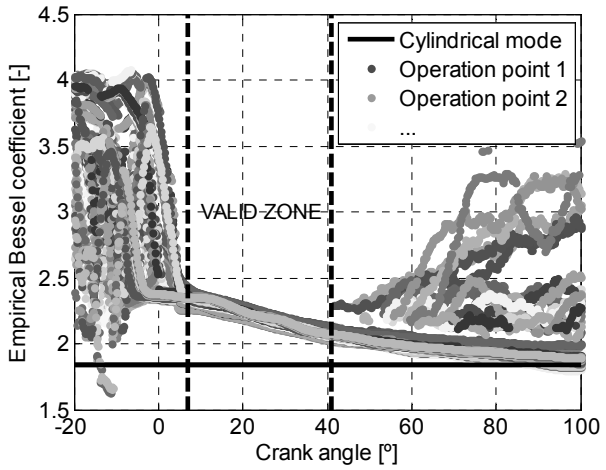

Figure 5. Empirical Bessel constants for the first mode ($B'_{1,0}$) obtained

Theoretically, if the mass is properly calculated all the Bessel constants obtained must coincide, regardless of the operation point, as they are only function of the geometry [16]. The calibration shows that the range for the method application must be between 10 and 40 degrees for the tested engine and combustion modes. In this range the combustion has started and properly excited the chamber resonance. Before 10 CAD, there is a significant risk of including sections of the pressure trace where there is neither combustion nor resonance, which shifts the results of the STFT. After 40 CAD the resonance dampening in some cases causes problems for determining the resonance frequency. Despite the high errors on this late zone, the tendency to converge to the cylindrical solution is evidenced far from the TDC.

Mass estimation

Steady operation

The resonance method was proved under 54 operation points, measuring 100 cycles at each point. For evaluating the resonance magnitude, the Ringing Intensity (RI) coefficient developed by Eng [24] was used:

$$RI = \frac{1}{2\gamma}\frac{\left(0.05\frac{\partial p}{\partial t_{max}}\right)}{p_{max}}\sqrt{\gamma R T_{max}} \qquad (14)$$

where the pressure gradient should be given in kPa/ms and the pressure in MPa in order to obtain MW/m^2.

The limit for a secure HCCI combustion is normally settled at 5MW/m^2 [25], while the noise is recognized at intensities of 4MW/m^2 [24]. Figure 6 shows that the points tested are normally under the audible limit and only some of them are classified as an abnormal combustion.

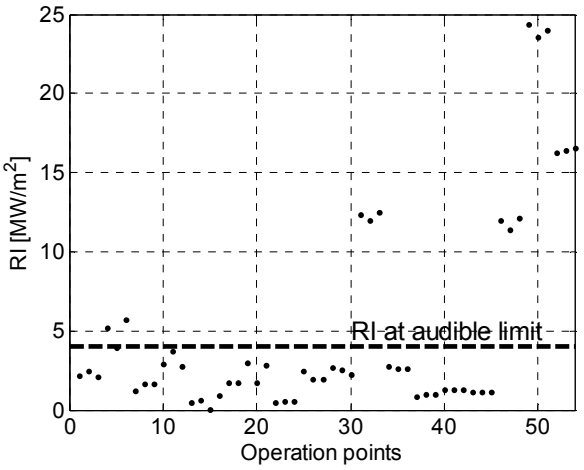

Figure 6. Empirical Bessel constants for the first mode ($B'_{1,0}$) obtained

Figure 7 shows the results in the mass estimation for three different cycles and the mean over 100 consecutive cycles. The mass flow is independently estimated for each crankshaft position (with a 0.2 degree step). As expected for the case when there is no significant blow-by, the mass estimation is almost constant during the expansion stroke, regardless of the crank angle position considered (α).

Significant intra-cycle differences of mass should permit detecting inaccurate points. For that, the standard deviation of the mass estimations during the n-th cycle is considered as an error metric of the measurement:

$$\varepsilon = \sqrt{\frac{\sum_\alpha (m_\alpha - \bar{m}_\alpha)^2}{N_\alpha - 1}}\frac{100}{\bar{m}_\alpha}(\%) \qquad (15)$$

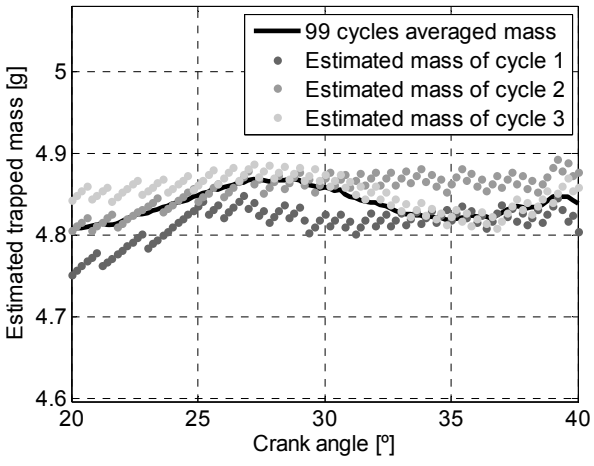

Figure 7. Intra-cycle mass estimations over different cycles in the same operation point.

Figure 8 shows the mean estimation and the intra-cycle standard deviation $\boldsymbol{\varepsilon}$ for each one of the 99 consecutive cycles at a given operation point. Although the measurement was conducted under steady conditions, small cycle-to-cycle deviations exist. These deviations might be caused by measurement errors, or also by stochastic processes associated with the engine operation. Cycle-to-cycle deviation was evaluated through:

$$\boldsymbol{\sigma} = \sqrt{\frac{\sum_n (\boldsymbol{m_n} - \bar{\boldsymbol{m}}_n)^2}{\boldsymbol{N_n - 1}}} \frac{\boldsymbol{100}}{\bar{\boldsymbol{m}}_n} (\%) \qquad (15)$$

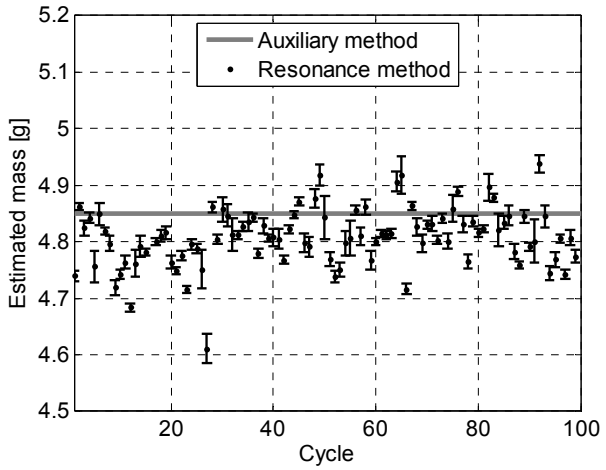

Figure 8. 100 cycles over a RCCI operation with one diesel injection at 50% load.

Table 3 sums up the different deviation metrics for all the operation points. The cycle-to-cycle deviations are within the expected range for the considered experimental setup, and the intra-cycle deviations shows that there are no significant changes in mass over any cycle.

Figure 9 shows the comparison between the auxiliary method and the pressure resonance method illustrating a very good agreement with the auxiliary method.

Table 3. Summary of resonance method results over the 54 stationary points (averaged over 100 cycles).

	minimum	average	maximum
Intra-cycle error % (ε)	0.25	0.45	1.05
Cyclic deviations % (σ)	0.55	1.41	2.86

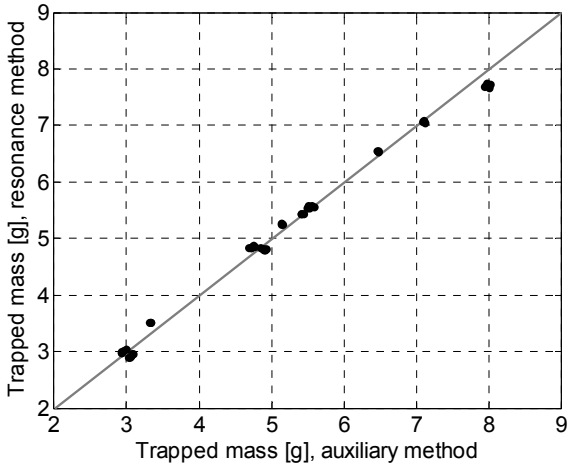

Figure 9. Trapped mass estimations over stationary points

Valve steps

In order to demonstrate the transient performance of the method, valve timing steps were conducted over different loads. The IVC was varied up to 45º (figure 10), letting the engine approximately one minute to ensure stabilization.

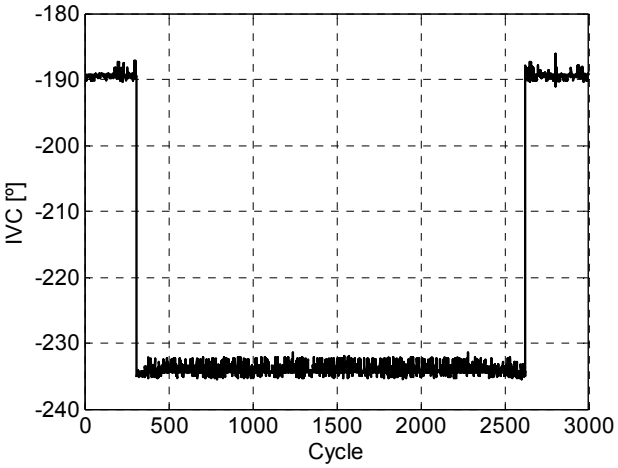

Figure 10. IVC change over a transient test

The sensor values were recorded and the mass was calculated with the auxiliary method. However, as this method is not able to compute the instantaneous mass during transients, only the averaged value of the trapped mass after it was stabilized was considered.

In contrast, the resonance method is perfectly fitted for obtaining one cycle resolution with a good precision. Figure 11 shows the output of the calculation compared with two levels measured by valve models. The shown signal considers a 10-cycle moving window for filtering cycle-to-cycle deviations and measurement noise.

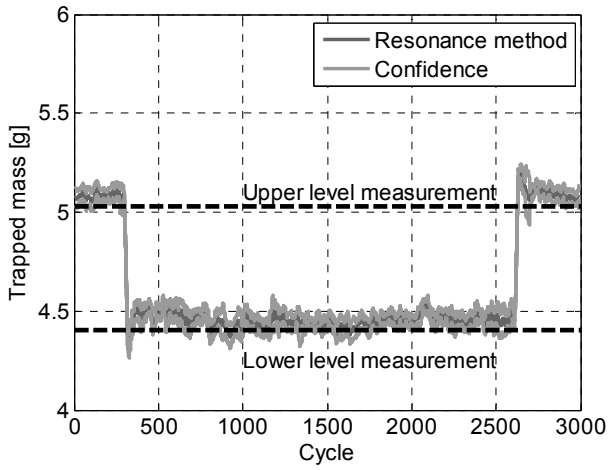

Figure 11. Mass obtained by the resonance method over the IVC step shown at figure 9 (50% load, 1200 rpm, RCCI one injection).

The mass calculations over every cycle were similar, and all the cycles had intra-cycles errors (ε) bellow 5%, as shown in Figure 12. The averaged error for all the cycles was 0.8%.

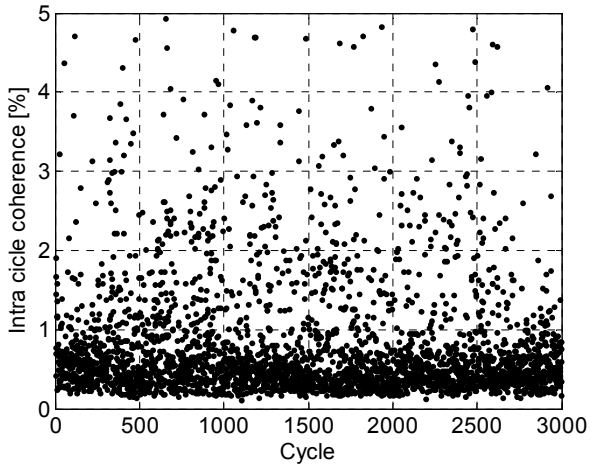

Figure 12. Intra-cycle errors (ε) obtained during the step test.

Conclusions

A method for estimating the in-cylinder trapped mass has been developed. The method relies on the pressure resonance phenomenon to obtain the speed of sound evolution during a cycle. Consequently, the speed of sound measurement only depends on the pressure signal and a pre-calculated Bessel parameter, which is only function of the cylinder geometry. The final mass measurement can be obtained by a rough estimation of γ and R (considering the composition constant) or by using polynomial expression for both magnitudes and computing a solvable state of equations (4-8). The method was tested on a single-cylinder RCCI engine under steady and transient conditions, showing one cycle resolution and coherent measures.

The errors associated to the constant composition assumption have been bounded below 1.1%. Nevertheless, assuming a constant composition would permit a trapped mass estimation by just the pressure signal and a crank angle reference (for the volume calculation).

In the author's opinion the main contributions of the presented method are:

- Lack of averaged values: The utilization of instant signals, such as the pressure, allows the method to obtain one cycle resolution at each cylinder (in multiple-cylinder engines).
- Few sources of errors: The method basically uses the pressure signal and a volume estimation, then only errors at these signals will affect the final measurement.
- One cycle error metrics: The possibility of many mass measures under the same cycle permits discarding wrong calculations.

As the method accuracy is affected by the frequency resonance identification, engines with low pressure gradients may have problems for the effective application of the method.

The method presents a good potential for engine control, as it provides a fast and reliable measurement of the trapped mass involving very few signals and a limited calculation power. More critical aspect for its final implementation is related with the sampling frequency requirements.

References

1. Chauvin, J., Corde, G., Vigild, C, Petit, N. et al., "Air Path Estimation on Diesel HCCI Engine", SAE Technical Paper 2006-01-1085, 2006, doi: 10.4271/2006-01-1085
2. Andersson, P. and Eriksson, L., "Air-to-Cylinder Observer on a Turbocharged SI-Engine with Wastegate", SAE Technical Paper 2001-01-0262, 2001, doi: 10.4271/2001-01-0262
3. Hockerdal, E., Eriksson, L. and Frisk, E., "Air Mass-Flow Measurement and Estimation in Diesel Engines Equipped with GR and VGT", SAE Technical Paper 2008-01-0992, 2008, doi: 10.4271/2008-01-0992
4. Pavkovic, D., Deur J., Kolmanovsky, I., and Hrovat, D.," Application of Adaptive Kalman Filter for Estimation of Power Train Variables", SAE Technical Paper 2008-01-0585, 2008, doi: 10.4271/2005-01-0036
5. Fantini, J., Peron, L. and Marguerie, B.," Identification and Validation of an Air Mass Flow Predictor Using a Nonlinear Stochastic State Representation", SAE Technical Paper 2000-01-0935, 2000, doi: 10.4271/2000-01-0935
6. Van Nieuwstadt, M.J., Kolmanovsky, I.V., Moraal, P.E., Stefanopoulou, A. et al." EGR-VGT control schemes: experimental comparison for a high-speed diesel engine". In *IEEE Control Systems Magazine*, volume 20, pages 64–79, 2000, doi: 10.1109/37.845039
7. De Cristofaro, F., Petrella, A., Cardone, M., Lanzilli, G. et al. "Air mass flow prediction algorithm". In *IEEE International Symposium on Industrial Electronics*, volume I, pages 265–268, 2005, doi: 10.1109/ISIE.2005.1528923.
8. Beltrami, C., Chamaillard, Y., Millerioux, G., Higelin, P. et al, "AFR control in SI engine with neural prediction of

cylinder air mass". In *Proceedings of the American Control Conference*, volume 2, pages 1404–1409, 2003, doi:10.1109/ACC.2003.1239787
9. Macián, V., Luján, J. M., Guardiola, C., and Perles, A.," A comparison of different methods for fuel delivery unevenness detection in Diesel engines", In *Mechanical Systems and Signal Processing*, volume 20, Issue 8, pages 2219–2231, 2006. doi:10.1016/j.ymssp.2005.04.001
10. Payri, F., Luján, J. M., Guardiola, C., and Rizzoni. G.," Injection diagnosis through common-rail pressure measurement", In *Proceedings of the Institution of Mechanical Engineers, Part D: Journal of Automobile Engineering*, Volume 220, Issue 3, Pages 347-357, 2006, doi: 10.1243/09544070JAUTO34
11. Payri, F., Galindo, J. , Martín, J. and Arnau, F.J, "A Simple Model for Predicting the Trapped Mass in a DI Diesel Engine", SAE Technical Paper 2007-01-0494, 2007, doi: 10.4271/2007-01-0494
12. Fox, J.W., Cheng, W. K. and Heywood J. B., "A Model for Predicting Residual Gas Fraction in Spark-Ignition Engines", SAE Technical Paper 931025, 1993, doi:10.4271/931025
13. Senecal, P. K., Xin, J. and Reitz R. D., "Predictions of Residual Gas Fraction in IC Engines", SAE Technical Paper 962052, 1996, doi:10.4271/962052
14. Desantes, J. M. , Galindo, J., Guardiola, C., and Dolz V., "Air mass flow estimation in turbocharged diesel engines from in-cylinder pressure measurement", In *Experimental Thermal and Fluid Science,* Volume 34, Issue 1, Pages 37-47, 2010, doi: 10.1016/j.expthermflusci.2009.08.009
15. Payri, F., Molina, S., Martín, J. and Armas, O., "Influence of measurement errors and estimated parameters on combustion diagnosis", In *Applied Thermal Engineering*, Volume 26, Issue 2-3, Pages 226-236, 2006, doi:10.1016/j.applthermaleng.2005.05.006
16. Hickling, R., Douglas, A., Feldmaier, F., Chen, H. K. et al., "Cavity resonances in engine combustion chambers and some applications", In *Journal of the Acoustical Society of America*, Volume 73, Issue 4, Pages 1170-1178, 1983, doi: 10.1121/1.389261
17. Hickling, R., Hamburg, J.A., Feldmaier, D.A. and Chung. J.Y., "Method of measurement of bulk temperatures of gas in engine cylinders. US PATENT, 1979.
18. Samimy, B. and Rizzoni, G., "Mechanical Signature Analysis Using TimeFrequency Signal Processing: Application to Internal Combustion Engine Knock Detection", In *Proceedings of the IEEE*, Volume 84, Issue 9, Pages 1330-1343, 1996, doi: 10.1109/5.535251
19. Corti, E. and Moro, D., " Knock Indexes Thresholds Setting Methodology", SAE Technical Paper 2007-01-1508, 2007, doi: 10.4271/2007-01-1508
20. Cavina, N., Corti, E., Minelli, G., Moro, D. et al.," Knock Indexes Normalization Methodologies", SAE Technical Paper 2006-01-2998, 2006, doi: 10.4271/2006-01-2998
21. Zhen, X., Wang, Y., Xu, S., Zhu, Y. et al., "The engine knock analysis - An overview", In *Applied Energy*, Volume 92, Pages 628-636, 2012, doi:10.1016/j.apenergy.2011.11.079
22. Draper. C.S., "The physical effects of detonation in a closed cylindrical chamber", Technical report, National Advisory Committee for Aeronautics, 1938.
23. Torregrosa, A. J., Broatch, A., Margot, X., Marant, V. et al., "Combustion chamber resonances in direct injection automotive diesel engines: A numerical approach", In *International Journal of Engine Research*, Volume 5, Issue 1, Pages 83-91, 2004, doi: 10.1243/146808704772914264
24. Eng, J.A., "Characterization of Pressure Waves in HCCI Combustion", SAE Technical Paper 2002-01-2859, 2002, doi: 10.4271/2002-01-2859
25. Sjöberg, M. and Dec, J.E., "Effects of Engine Speed, Fueling Rate, and Combustion Phasing on the Thermal Stratification Required to Limit HCCI Knocking Intensity", SAE Technical Paper 2005-01-2125, doi: 10.4271/2005-01-2125
26. Lu, X., Han, D. and Huang, Z., " Fuel design and management for the control of advanced compression-ignition combustion modes", In *Progress in Energy and Combustion Science*, Volume 37, Issue 6, Pages 741-783, 2011, doi: 10.1016/j.pecs.2011.03.003
27. Lapuerta, M., Armas, O. and Hernández, J. J., "Diagnosis of DI Diesel combustion from in-cylinder pressure signal by estimation of mean thermodynamic properties of the gas", In *Applied Thermal Engineering*, Volume 19, Issue 5, Pages 513-529, 1999, doi: 10.1016/S1359-4311(98)00075-1
28. Brunt, M. and Emtage, A., "Evaluation of Burn Rate Routines and Analysis Errors", SAE Technical Paper 970037, 1997, doi: 10.4271/970037
29. Joint Committee for Guides in Metrology (JCGM), "Evaluation of Measurement Data - Guide to the Expression of Uncertainty in Measurement", Technical Report, JCGM, 2008.

Definitions/Abbreviations

CA50	Crank Angle where is released the 50% of the heat
ECU	Electronic Control Unit
HCCI	Homogenous Charge Compression Ignition
IVC	Intake Valve Closing
MFB	Mass Fraction Burnt
RCCI	Reactivity Controlled Compression Ignition
SOC	Start Of Combustion
TDC	Top Dead Center
VVT	Variable Valve Timing

Appendix A. Mass error propagation throw composition

The maximum error at the mass due to composition was estimated from equation (6) by applying linear error propagation [29]:

$$\varepsilon(m) = \left|\varepsilon(pV)\frac{\partial(m)}{\partial(pV)}\right| + \left|\varepsilon(RT)\frac{\partial(m)}{\partial(RT)}\right| = \left|\frac{\varepsilon(pV)}{RT}\right| + \left|\frac{\varepsilon(RT)pV}{(RT)^2}\right| \quad \text{(A.1)}$$

$$\frac{\varepsilon(m)}{m} = \left|\frac{\varepsilon(pV)}{pV}\right| + \left|\frac{\varepsilon(RT)}{RT}\right| = \left|\frac{\varepsilon(pV)}{pV}\right| + f(a, Y_x) \quad \text{(A.2)}$$

The maximum error committed at $\left|\frac{\varepsilon(RT)}{RT}\right|$ is the maximum difference caused by Y_x for each possible value of a. The possible limits of a and Y_x where selected as the limits findable in a cylinder of an alternative combustion engine (A.3): The composition was bounded between 0% air (complete stoichiometric combustion) and 100% air (the poorest possible mix), disregarding the effect of the fuel for dimensional simplicity.

$$a \rightarrow [400{,}1000]\ m/s$$

$$Y_a \rightarrow [0{,}1] \quad \text{(A.3)}$$

Figure 12 (left) illustrate the effect of the composition and the speed of sound over RT (the composition has almost no effect), while figure 12 (right) bounds the effect of the composition for each speed of sound (grey scale lines) between 1.7% and -1.8%. As conclusion, the assumption of having 50% of burnt products and 50% of air over all the cycle only distort the measurement between 1.7% and -1.8% (extreme cases).

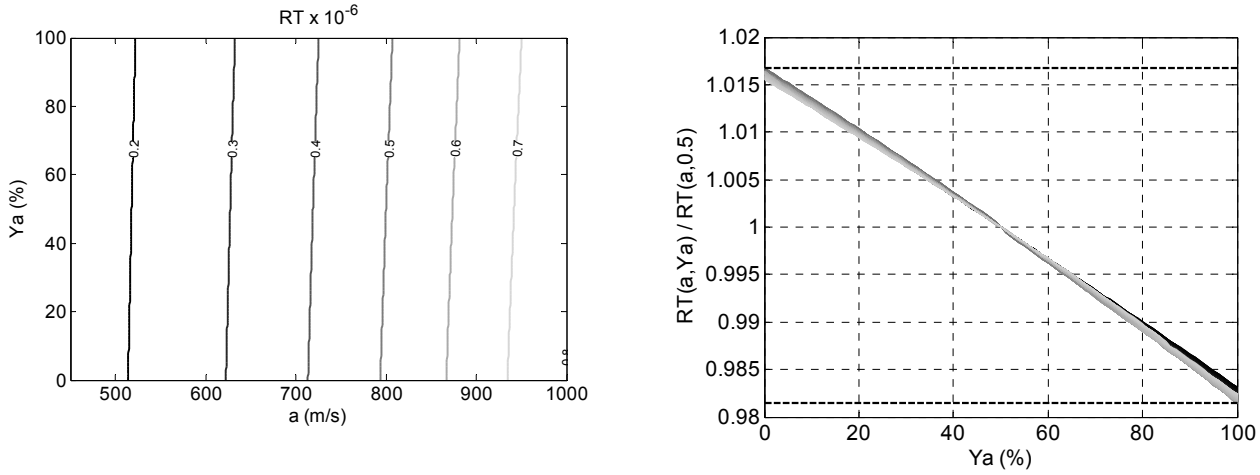

Figure 12. RT variation due to composition and speed of sound (left), and effect of the composition on the mass for every value of speed of sound (right)